Effect of pinning particles on grain boundary motion from interface random walk

Dengke Chen, Tarek Ghoneim, and Yashashree Kulkarni

Citation: Appl. Phys. Lett. **111**, 161606 (2017); doi: 10.1063/1.4986294
View online: http://dx.doi.org/10.1063/1.4986294
View Table of Contents: http://aip.scitation.org/toc/apl/111/16
Published by the American Institute of Physics

Effect of pinning particles on grain boundary motion from interface random walk

Dengke Chen, Tarek Ghoneim, and Yashashree Kulkarni[a)]
Department of Mechanical Engineering, University of Houston, Houston, Texas 77204, USA

(Received 3 June 2017; accepted 5 October 2017; published online 20 October 2017)

Impurities can dramatically influence grain boundary migration, thereby impacting material properties. In this letter, we present a theoretical model for grain boundary motion in the presence of embedded particles using the interface random walk approach. Based on the fluctuation-dissipation relation, we derive an analytical expression relating the grain boundary fluctuations to the boundary mobility and key parameters governing the drag effect of the particles. In addition to predicting the modified boundary mobility due to pinning particles, the model provides a way to estimate the force acting on the particle-boundary interface from atomistic simulations. The theory facilitates an enriched analysis of atomistic simulations of a grain boundary with embedded particles, revealing that a pinned grain boundary exhibits a response akin to tethered Brownian motion. *Published by AIP Publishing.* https://doi.org/10.1063/1.4986294

As interfaces are ubiquitous in materials, interfacial phenomena play a vital role in engineering microstructures for desired material properties.[1–3] Specifically, it is grain boundary migration, or more broadly, motion of interfaces, that drives microstructural evolution and sets the final configuration of interfaces during materials processing. Here, migration refers to the motion of the grain boundary normal to its plane. A key parameter that determines grain boundary kinetics and accounts for the effect of the boundary structure, temperature, and the atomistic environment is the grain boundary mobility. Mobility M relates the normal velocity v of the grain boundary to the driving force p through the well-known relation $v = Mp$ and is known to be dramatically impacted by the presence of impurities, such as interstitials, defect clusters, and second phase particles, sometimes by several orders of magnitude.[4,5] In fact, the large discrepancies found between mobilities predicted by modeling (of perfect interfaces) and those estimated from experiments are attributed to the drag effect of impurities invariably present in experimental specimens. Naturally then, grain boundary mobility[6–15] and the drag effect of impurities[3,16–26] have been the subject of active research over the past few decades. Since controlled experiments on the normal motion of individual grain boundaries are difficult to perform, critical insights into the role of impurities have mostly been obtained by way of theoretical analyses, such as the well-known CLS (Cahn-Lücke-Stüwe) model,[16,17] and the Zener pinning model,[18,19] and more recently, atomistic simulations.[21–24,26,27] A majority of this work is based on the CLS model for impurity particles which uses a simplistic triangular potential to describe the boundary-particle interaction energy but is lacking in mechanistic details of the interaction. In this regard, the Zener pinning model, which accounts for the size-dependent drag effect of particles, provides novel insights into the interaction between impurities and the grain boundary. However, the focus of the Zener pinning studies has largely been on macroscopic grain growth rather than on mobility of individual grain boundaries.

In this article, we present a fresh perspective and theoretical approach, based on thermal fluctuations, for grain boundary motion that proffers mechanistic insights into the microscopic interaction between grain boundary and pinning impurities. Among other insights, it facilitates an enriched analysis of our molecular dynamics (MD) simulations of fluctuating grain boundaries with embedded particles. Combining the interface random walk approach[11] and ideas from the Zener pinning model,[18] we derive the modified grain boundary diffusion equation in terms of the boundary mobility and key parameters governing the drag effect of the particles. We regard the motion of the boundary with pinning particles as a Brownian motion with restoring force and propose a simple and efficient calculation method to obtain the modified boundary mobility. Using this model in conjunction with a series of MD simulations, we obtain the mobility of a symmetric tilt grain boundary with particles. The simulation results provide validation for the theoretical model and shed light on the role of particle density, size, and temperature in the drag effect of the particles. In the context of this work, we use ideas from the Zener theory as a way to describe the interaction between the grain boundary and the pinning particles within the framework of the interface random walk approach. In that aspect, our central idea is similar to the work of Hillert[20] (and some recent works[25,26]) where the Zener pinning model is applied to take into account the effect of second-phase particles on grain growth and boundary migration. Thus, in what follows, the phrase "pinning effect" does not imply that the pinned grain boundary is immobile. It merely conveys that the embedded particles exert a (drag or pinning) force that retards grain boundary normal motion.

We adopt the interface random walk method proposed by Trautt *et al.*[11] and extended to low temperatures by Deng and Schuh[13] to estimate the boundary mobility. This method extracts the mobility of the boundary from its out-of-plane thermal fluctuations and thereby eliminates the need for applying large external driving forces to simulate actual boundary migration.[12] Here, the mean boundary displacement, $\bar{h}(t)$, defined as the average displacement of every atom residing in the grain boundary in the migration direction at time t,

[a)]Electronic mail: ykulkarni@uh.edu

is considered as exhibiting Brownian motion due to thermal fluctuations. Thus, applying the fluctuation-dissipation relation, the grain boundary diffusion equation in terms of the variance, $\langle \bar{h}^2(t) \rangle$, is derived as $\langle \bar{h}^2(t) \rangle = \frac{2Mk_BT}{A}t$, where A is the area of the boundary and $D = \frac{2Mk_BT}{A}$ is the diffusion coefficient. Mobilities determined from this equation have been shown to be consistent with those obtained from other MD simulation approaches based on driving forces.[6–8] Over the past decade, the interface random walk method has been successfully applied to estimate the mobility of impurity-free grain boundaries[11,13,14] and boundaries with impurity atoms.[23,24]

To account for embedded particles in the above method, we treat the normal motion of a grain boundary with pinning particles as Brownian motion with restoring force. We first note that the diffusion of the particles considered in our study over a range of temperatures is negligible. This is consistent with the classic Stokes-Einstein relation and also verified by atomistic simulations (described in detail in the supplementary material). Thus, in what follows, we do not distinguish between the absolute displacement of the grain boundary and its relative displacement with respect to the particles.

The schematic in Fig. 1(c) illustrates the central idea of our theoretical model. As the boundary migrates from the equilibrium position (indicated by the dashed blue line) to a new position (indicated by the wavy dashed red line), it experiences a restoring force (due to the particles) that pulls it back to the equilibrium position. This force may be thought of as a "spring" force between the boundary and the particles. Applying the Zener pinning model to this quasi one-dimensional problem, the force acting on the particle-boundary interface is considered to be proportional to the mean boundary displacement $\bar{h}$ and the interfacial tension.[18,19] Hence, we assume the interaction energy between the boundary and the particle, ΔE, to have a quadratic dependence on the mean boundary displacement

$$\Delta E(\bar{h}) = \frac{1}{2}Ak_s\bar{h}^2, \tag{1}$$

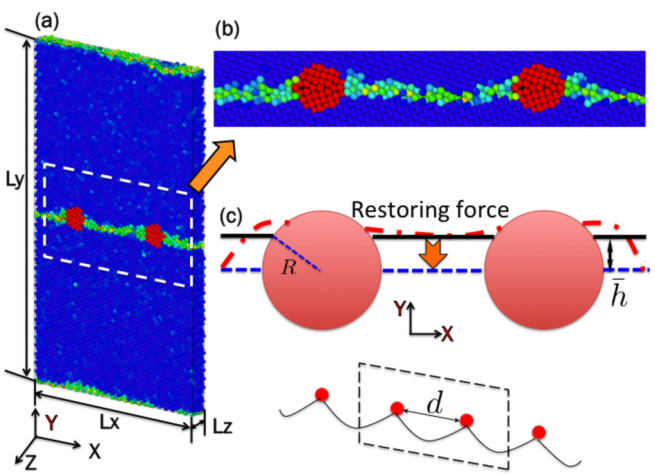

FIG. 1. (a) Atomistic configuration of the MD simulation cell visualized using OVITO.[33] (b) Atomistic structure of a fluctuating grain boundary with embedded particles (red atoms) with spacing d. (c) Schematic showing the drag effect of particles on the grain boundary.

where A is the area of the grain boundary and k_s is defined as the drag coefficient arising from the pinning particle. Thus, the drag force is defined as

$$f_r = -\frac{1}{A}\frac{\partial \Delta E}{\partial \bar{h}} = -k_s\bar{h} \tag{2}$$

and is proportional to $\bar{h}$. The drag coefficient k_s is a composite parameter that depends on various factors, including the interfacial tension, temperature, particle radius, and particle spacing, the details of which are deferred to later discussion. Following the interface random walk approach,[11] we start with the relation $v = Mp$ where $v = h_t$, and the driving force p comprises the capillary force that arises due to curvature, the Langevin force due to thermal fluctuations, and the drag force. Spatially averaging this relation yields $\bar{h}_t = M[\bar{\xi}(t) - k_s\bar{h}(t)]$, where the spatial average of the capillary force vanishes due to periodicity and the average of the thermal noise is denoted by $\bar{\xi}(t)$. Integrating this equation in time, the modified boundary diffusion equation becomes

$$\begin{aligned}\langle \bar{h}^2(t) \rangle &= \frac{k_BT}{Ak_s}(1 - e^{-2Mk_st}) \\ &= \begin{cases} \dfrac{2Mk_BT}{A}t & \text{if } t \ll \dfrac{1}{Mk_s} \\ \dfrac{k_BT}{Ak_s} & \text{if } t \gg \dfrac{1}{Mk_s}. \end{cases}\end{aligned} \tag{3}$$

The derivation is provided in the supplementary material. Equation (3) illustrates that the grain boundary with embedded particles performs a classical random walk initially such that $\langle \bar{h}^2 \rangle$ increases linearly with time and then approaches a constant value of $\frac{k_BT}{Ak_s}$ due to the presence of the particles. Thus, the model proposes that a pinned grain boundary exhibits a viscous-like response akin to tethered particle motion, a well-studied biophysical experimental method which tracks a Brownian particle attached to a substrate by a polymer.[28,29]

For validation, we perform MD simulations to compute the mobility of two [001] symmetric tilt grain boundaries,[30] $\Sigma5(310)$ and $\Sigma17(410)$, with misorientation angles of 36.87° and 28.07°, respectively, in Nickel. The results for both boundaries are consistent with the above analytical predictions. Hence, we discuss the $\Sigma5$ grain boundary results here to compare our work with prior studies based on the similar grain boundary structure, while the simulations for the $\Sigma17$ grain boundary are relegated to the supplementary material. Each grain boundary is embedded with an array of particles with varying spacing d. The size of the simulation cell is 13.3 nm × 22.2 nm × 1.0 nm, and the radius of the embedded particles is $R = 0.44$ nm [Fig. 1(a)]. The cylindrical-shaped particles also consist of Ni atoms but are specified to be rigid clusters [Fig. 1(b)]. The embedded-atom (EAM) interatomic potential by Ackland *et al.*[31] is used with periodic boundary conditions in X and Z directions. The system is free to relax in the Y direction, which is normal to the boundary. The residual stress around the rigid clusters is removed by using the "heating-and-quenching" approach outlined by Deng and Schuh.[14] The sample is then equilibrated for 2 ns under the NVT ensemble using the Nose-Hoover

thermostat. Two thin slabs of atoms are fixed at the top and bottom surfaces to prevent rigid motion of the simulation cell. Using the approach described elsewhere[34,35] (see supplementary material), we extract the instantaneous profile of the grain boundary using the centrosymmetry parameter and determine its mean displacement $\bar{h}(t)$. The mean displacement distribution and ensemble variance are calculated by performing multiple simulations in parallel. The simulations are performed at temperatures ranging from 900 K to 1200 K, using LAMMPS.[32]

Figure 2 plots the evolution of $\bar{h}(t)$ of the $\Sigma5(310)$ boundary with particles at 1000 K. The distribution is Gaussian at each time interval confirming that the fluctuating grain boundary exhibits a random walk even in the presence of particles. More importantly, the spread of $\bar{h}(t)$ initially increases over time and then remains constant beyond a certain time ($\alpha_{10} = 3.87 > \alpha_{20} = 2.64 > \alpha_{400} = 1.23 \approx \alpha_{800} = 1.22$). In fact, the distributions at 400 ps and 800 ps are almost identical ($B_{400} = 248 \approx B_{800} = 247$). This is consistent with our theoretical prediction. Furthermore, as illustrated in Fig. 3(a), $\langle \bar{h}^2 \rangle$ obtained from MD simulations obeys the trend predicted by Eq. (3) (solid lines) at different temperatures. Thus, the simulations reveal that a pinned grain boundary indeed exhibits tethered Brownian motion as proposed by the model. In Fig. 3(a), Eq. (3) is fitted separately to simulation data for a specific temperature, particle radius, and particle spacing to obtain the boundary mobilities and the drag coefficients. We note that even in the presence of particles, the mobility increases with temperature, by a factor of around 30 from $M = 3.33 \times 10^{-9} \mathrm{m^2 J^{-1} s^{-1}}$ at 900 K to $M = 9.30 \times 10^{-8} \mathrm{m^2 J^{-1} s^{-1}}$ at 1200 K. Figure 3(b) compares the simulation results at 1000 K for varying particle spacings. For clarity, we only show the evolution of $\langle \bar{h}^2 \rangle$ during the first 50 fs when it increases linearly and the slope gives the mobility. It is evident that the presence of particles can decrease the boundary mobility. Figure 3(c) shows the semilog plot for M versus $1/k_BT$ for different particle spacings. In order to obtain better fitting, we performed more simulations at intermediate temperatures, specifically, 925, 950, 975, 1050, and 1150 K. As expected, the mobility follows the Arrhenius relation, $M \propto \exp\left(-\frac{Q_m}{k_B T}\right)$, albeit with two distinct regimes having different activation energies Q_m. The different regimes, also reported in prior works, correspond to a transition in grain boundary motion, and this is attributed

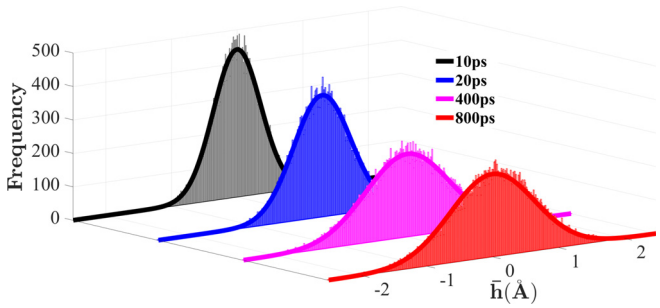

FIG. 2. Distribution of $\bar{h}(t)$ of $\Sigma5$ boundary at t = 10, 20, 400, and 800 ps at 1000 K with particle spacing $d = 6.7$ nm. The functions $f = Be^{-\alpha \bar{h}^2}$ are fitted to the Gaussian distribution form (solid lines), where the B and α are measures of the height and width of the distribution, respectively.

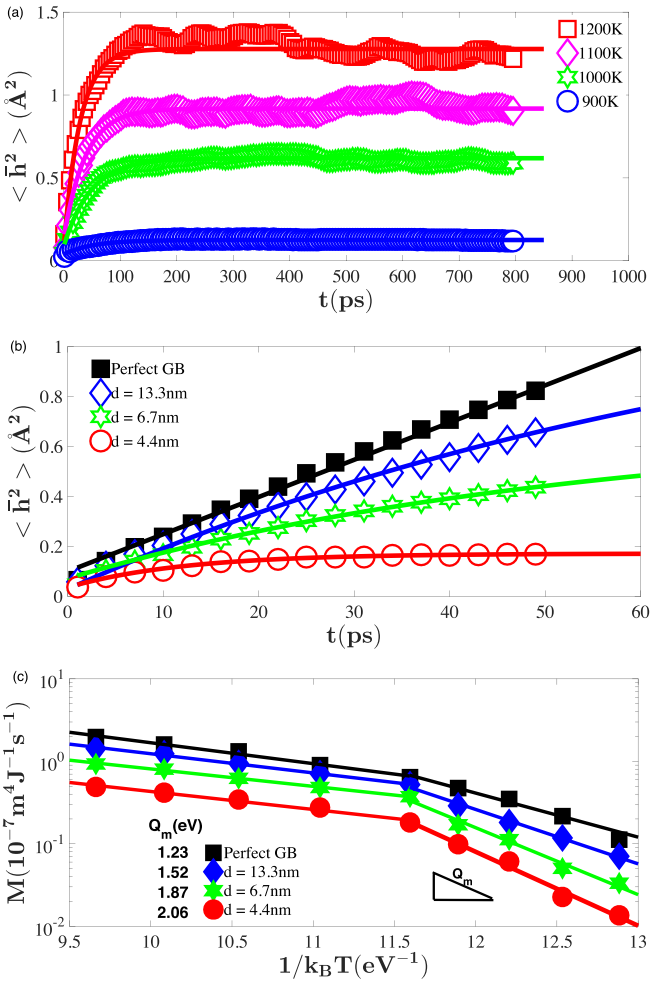

FIG. 3. Time evolution of the variance of the mean boundary displacement ($\langle \bar{h}^2 \rangle$) (a) at different temperatures with particle spacing $d = 6.7$ nm; (b) at 1000 K, with varying particle spacings. (c) Semilog plot for M versus $1/k_BT$ showing a piecewise Arrhenius relation with different activation energies Q_m. The grain boundary is $\Sigma5$ and the particle radius is $R = 0.44$ nm.

to structural transitions in the boundaries as they exhibit a more liquid-like behavior above the transition temperature.[13,36,37] From Fig. 3(c), we note that Q_m changes negligibly with varying particle densities above the transition temperature. This may also be due to the liquid-like behavior of the grain boundary which makes the pinning effect of the particles weaker. Specifically, the case with no particles gives fairly consistent values for mobilities compared with the results reported by Deng and Schuh.[13] There is also a good agreement between the two studies for the activation energy (1.23 eV (present work) $\sim$ 1.16±0.08 eV [13]). Below the transition temperature, decreasing the particle spacing increases the activation energy for migration from 1.23 eV for the perfect grain boundary to 2.06 eV with particle spacing $d = 4.4$ nm which is expected. At 900 K, $M = 1.35 \times 10^{-9} \mathrm{m^2 J^{-1} s^{-1}}$ for $d = 4.4$ nm is an order of magnitude smaller than $M = 1.12 \times 10^{-8} \mathrm{m^2 J^{-1} s^{-1}}$ for the perfect grain boundary. This agrees very well with the results of Sun and Deng[23] for a similar temperature and similar grain boundary with impurity atoms. They report that the mobilities of a boundary with only 2 impurity atoms and a boundary with 61 impurity atoms differ by an order of magnitude. This agreement provides strong supporting evidence that our

fluctuation-based method furnishes reasonable values for boundary mobility in the presence of pinning particles (or clusters) when compared to simulations[23] in which the boundary mobility is reduced by impurity atoms that move with the grain boundary. Furthermore, this substantial decrease in mobility endorses the view that the discrepancy in grain boundary mobilities observed in simulations and experiments can be attributed to the presence of impurities in the latter.

The proposed model also opens an avenue for quantifying the drag effect of particles. As a first step, we present a qualitative discussion on estimating the drag coefficient since Eq. (3), in conjunction with MD simulations for $\langle \bar{h}^2 \rangle$ in the presence of particles, provides a convenient way to extract Ak_s. A more quantitative analysis would need comprehensive simulations using advanced computational methods, as explained below, coupled with a more sophisticated model for the drag effect (compared to Eq. (4) below), which are beyond the scope of this paper.

Dimensional analysis of Eq. (1) shows that Ak_s has the units of energy per unit area which is consistent with the interfacial free energy γ of the grain boundary. It is important to note that the interfacial free energy is thermodynamically relevant in the context of grain boundary motion because it is related to the interfacial tension which provides the driving force for curvature-driven normal motion of grain boundaries.[11,38] Consequently, the drag force due to a particle would also depend on the interfacial tension, or more generally, the interfacial free energy. According to the classical Zener pinning model, the drag force of a particle embedded in a grain boundary is linearly dependent on the interfacial tension.[18,19] We further reason that the drag force should depend on the ratio of the particle radius to spacing, i.e., R/d, which denotes the particle density in our quasi-1D grain boundary representation. This dependence on R/d, albeit with a different functional form, was also reported by Wang *et al.*[25] based on their phase field model for Zener pinning. Based on the general trend shown by our atomistic simulations, we propose the following power-law dependence of the drag coefficient on R/d:

$$Ak_s = \alpha\,\gamma(T)\left(\frac{R}{d}\right)^{\beta}, \tag{4}$$

where the effect of temperature is incorporated through $\gamma(T)$ which usually decreases with temperature.[38] α and β are fitting parameters. Using Eq. (3) and the simulation results for $\langle \bar{h}^2 \rangle$ from Fig. 3(a), the quantity Ak_s can be extracted from the limit $\frac{k_B T}{Ak_s}$. To explore the contribution of the different factors, we performed a series of simulations on larger specimens of size 28.6 nm × 22.2 nm × 1.0 nm and various particle radii, specifically, $R = 0.44$ nm, 0.55 nm, 0.66 nm, 0.83 nm and spacings, $d = 13.3$ nm, 6.7 nm, 4.4 nm.

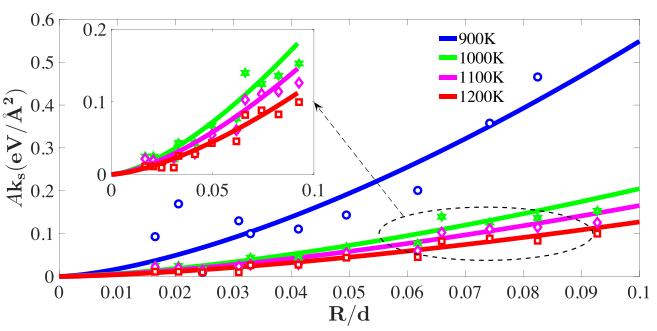

FIG. 4. The dependence of Ak_s on $\frac{R}{d}$ at different temperatures for the Σ5 grain boundary.

Figure 4 shows the MD results and the fitted curves for the dependence of Ak_s on the ratio R/d for different temperatures. We get a better fit at higher temperatures as shown in the inset. Based on our least squares fit, the exponent β for the Σ5 boundary is calculated to be 1.5 ± 0.3. For the Σ17 boundary, the β is estimated to be 1.8 ± 0.3 (see supplementary material). The simulation data for both grain boundaries show a reasonable fit with Eq. (4) with β between 1 and 2. We emphasize that the calculations for the drag coefficient are qualitative estimates which demonstrate that the power law relation proposed is a good starting point, although its physical underpinning is not yet clear to us. The factor α may be determined from the calculation of $\gamma(T)$ for the particular grain boundary which would entail using advanced computational tools and is beyond the scope of the present study. However, our MD results indicate that k_s can vary considerably with temperature. This is in agreement with the atomistic calculations by Foiles[38] which reveal that the interfacial free energy γ changes substantially with temperature. Thus, our approach can provide a preliminary estimation of the drag force of the embedded particles. However, we note that the actual interaction between the grain boundary and particles is quite complex and may depend on several factors such as the boundary structure, temperature, shape of the particles, and the mechanism of normal motion. Equation (4) is a fairly simplified phenomenological relation that captures the key characteristics of the drag effect and demonstrates the ability of our theoretical model to estimate the drag force based on the thermal fluctuations of the pinned grain boundary.

In summary, we propose a concise and effective method to elucidate the effect of embedded particles on grain boundary migration based on the interface random walk approach. The theory facilitates an enriched analysis of atomistic simulations of a grain boundary with embedded particles, revealing that a pinned grain boundary exhibits a response akin to tethered Brownian motion. In addition to predicting the modified boundary mobility, the model offers a way to estimate the force acting on the particle-boundary interface from atomistic simulations. As a first step, the effects of particle size, particle spacing, and temperature on the drag force are explored. Enriching the model with a more sophisticated boundary-particle interaction model and extending the analysis to the fully three-dimensional case, with say spherical particles, provide directions for further investigation. Finally, incorporating the breakaway of grain boundaries from strongly pinning particles into the mobility calculations forms an exciting avenue for future work.

See supplementary material for detailed derivation of Eq. (3), additional simulation details, and a summary of the MD results for the Σ17(410) symmetric tilt boundary.

We gratefully acknowledge the support of NSF under Grant Nos. CMMI-1129041 and DMR-1508484. The authors also acknowledge the use of the Maxwell Cluster and the support from the Center of Advanced Computing and Data Systems at the University of Houston to carry out the research presented here.

[1]A. P. Sutton and R. W. Balluffi, *Interfaces in Crystalline Materials* (Oxford, 1995).
[2]G. Gottstein and L. S. Shvindlerman, *Grain Boundary Migration in Metals: Thermodynamics, Kinetics, Applications* (CRC Press, 1999).
[3]M. I. Mendelev and D. J. Srolovitz, Modell. Simul. Mater. Sci. Eng. **10**, R79 (2002).
[4]D. Turnbull, Trans. AIME, Journal of Metals **191**, 661 (1951).
[5]J. W. Cahn and A. Novick-Cohen, Acta Mater. **48**, 3425 (2000).
[6]M. Upmanyu, D. J. Srolovitz, L. S. Shvindlerman, and G. Gottstein, Acta Mater. **47**, 3901 (1999).
[7]K. G. F. Janssens, D. Olmsted, and E. A. Holm, Nat. Mater. **5**, 124 (2006).
[8]S. M. Foiles and J. J. Hoyt, Acta Mater. **54**, 3351 (2006).
[9]G. Gottstein, D. A. Molodov, L. S. Shvindlerman, D. J. Srolovitz, and M. Winning, Curr. Opin. Solid State Mater. Sci. **5**, 9 (2001).
[10]F. Mompiou, D. Caillard, and M. Legros, Acta Mater. **57**, 2198 (2009).
[11]Z. T. Trautt, M. Upmanyu, and A. Karma, Science **314**, 632 (2006).
[12]J. J. Hoyt, Z. T. Trautt, and M. Upmanyu, Math. Comput. Simul. **80**, 1382 (2010).
[13]C. Deng and C. A. Schuh, Phy. Rev. Lett. **106**, 045503 (2011).
[14]C. Deng and C. A. Schuh, Phy. Rev. B **84**, 214102 (2011).
[15]M. I. Mendelev, C. Deng, C. A. Schuh, and D. J. Srolovitz, Modell. Simul. Mater. Sci. Eng. **21**, 045017 (2013).
[16]J. W. Cahn, Acta Metall. **10**, 789 (1962).
[17]K. Lucke and H. P. Stuwe, *Recovery and Recrystallization of Metals* (Interscience, New York, 1963).
[18]C. S. Smith, Trans. AIME **175**, 15 (1948).
[19]P. A. Manohar, M. Ferry, and T. Chandra, ISIJ Int. **38**, 913 (1998).
[20]M. Hillert, Acta Metall. **13**, 227 (1965).
[21]M. I. Mendelev and D. J. Srolovitz, Acta Mater. **49**, 589 (2001).
[22]M. I. Mendelev and D. J. Srolovitz, J. Mater. Res. **20**, 208 (2005).
[23]H. Sun and C. Deng, Comp. Mater. Sci. **93**, 137 (2014).
[24]H. Sun and C. Deng, J. Mater. Res. **29**, 1369 (2014).
[25]N. Wang, Y. Wen, and L.-Q. Chen, Comp. Mater. Sci. **93**, 81 (2014).
[26]R. K. Koju, K. A. Darling, L. J. Kecskes, and Y. Mishin, JOM **68**, 1596 (2016).
[27]A. T. Wicaksono, M. Militzer, and C. W. Sinclair, IOP Conf. Ser.: Mater. Sci. Eng. **89**, 012048 (2015).
[28]J. F. Beausang, C. Zurla, L. Finzi, L. Sullivan, and P. C. Nelson, Am. J. Phys. **75**, 520 (2007).
[29]S. Kumar, C. Manzo, C. Zurla, S. Ucuncuoglu, L. Finzi, and D. Dunlap, Biophys. J. **106**, 399 (2014).
[30]J. W. Cahn, Y. Mishin, and A. Suzuki, Acta Mater. **54**, 4953 (2006).
[31]G. J. Ackland, G. T. Tichy, V. V. Vitek, and M. W. Finnis, Philos. Mag. A. **56**, 735 (1987).
[32]S. J. Plimpton, J. Comp. Phys. **117**, 1 (1995).
[33]A. Stukowski, Modell. Simul. Mater. Sci. Eng. **18**, 015012 (2010).
[34]D. Chen and Y. Kulkarni, MRS Commun. **3**, 241 (2013).
[35]D. Chen and Y. Kulkarni, J. Mech. Phys. Solids **84**, 59 (2015).
[36]H. Zhang, D. J. Srolovitz, J. F. Douglas, and J. A. Warren, Proc. Natl. Acad. Sci. **106**, 7735 (2009).
[37]B. Schonfelder, P. Keblinski, D. Wolf, and S. R. Phillpot, Mater. Sci. Forum **294–296**, 9 (1999).
[38]S. M. Foiles, Scr. Mater. **62**, 231 (2010).